



**First-Row Transition Metal Complexes of ENENES Ligands:  
The Ability of the Thioether Donor to Impact the  
Coordination Chemistry**

Journal:	<i>Dalton Transactions</i>
Manuscript ID	DT-ART-10-2015-003855.R1
Article Type:	Paper
Date Submitted by the Author:	24-Nov-2015
Complete List of Authors:	Dub, Pavel; Los Alamos National Laboratory, Chemistry Scott, Brian; Los Alamos National Laboratory, Gordon, John; Los Alamos National Laboratory, Chemistry Division

# First-Row Transition Metal Complexes of ENENES Ligands: The Ability of the Thioether Donor to Impact the Coordination Chemistry

Pavel A. Dub,<sup>\*,||</sup> Brian L. Scott<sup>‡</sup> and John C. Gordon<sup>\*,||</sup>

<sup>||</sup>Chemistry Division and <sup>‡</sup>Materials and Physics Applications Division

Los Alamos National Laboratory

Los Alamos, New Mexico 87545, United States

[pdub@lanl.gov](mailto:pdub@lanl.gov); [jgordon@lanl.gov](mailto:jgordon@lanl.gov)

**Abstract.** The reactions of two variants of ENENES ligands,  $E(\text{CH}_2)_2\text{NH}(\text{CH}_2)_2\text{SR}$ , where E = 4-Morpholinyl, R = Ph (**a**), Bn (**b**) with  $\text{MCl}_2$  (M = Mn, Fe, Co, Ni and Cu) in coordinating solvents (MeCN, EtOH) affords isolable complexes, whose magnetic susceptibility measurements suggest paramagnetism and a high-spin formulation. X-Ray diffraction studies of available crystals show that the ligand coordinates to the metal in either a bidentate  $\kappa^2[\text{N},\text{N}']$  or tridentate  $\kappa^3[\text{N},\text{N}',\text{S}]$  fashion, depending on the nature of ligand and/or identity of the metal atom. In the case of a less basic SPh moiety, a bidentate coordination mode was identified for harder metals (Mn, Fe), whereas a tridentate coordination mode was identified in the case of a more basic SBn moiety with softer metals (Ni, Cu). In the intermediate case of Co, ligands **a** and **b** coordinate via  $\kappa^2[\text{N},\text{N}']$  and  $\kappa^3[\text{N},\text{N}',\text{S}]$  coordination modes, which can be conveniently predicted by DFT calculations. For the softest metal (Cu), ligand **a** coordinates in a  $\kappa^3[\text{N},\text{N}',\text{S}]$  fashion.

**Introduction.** The vast majority of ligands used in homogeneous catalysis are based on P and/or N donor atoms, with an enormous number of such ligands having been designed and synthesized over the past five decades.<sup>1</sup> Among them are polydentate chelating ligands bearing N–H functionalities<sup>2</sup> that are currently accepted to play a crucial role in so-called “metal–ligand bifunctional catalysis”.<sup>3</sup> Representative examples of the commercially available PNP ligand family<sup>4</sup> of general formula  $R_2P(CH_2)_2NH(CH_2)_2PR_2$  are shown in Chart 1. Members of this ligand class have been known since the 1970’s.<sup>5</sup>

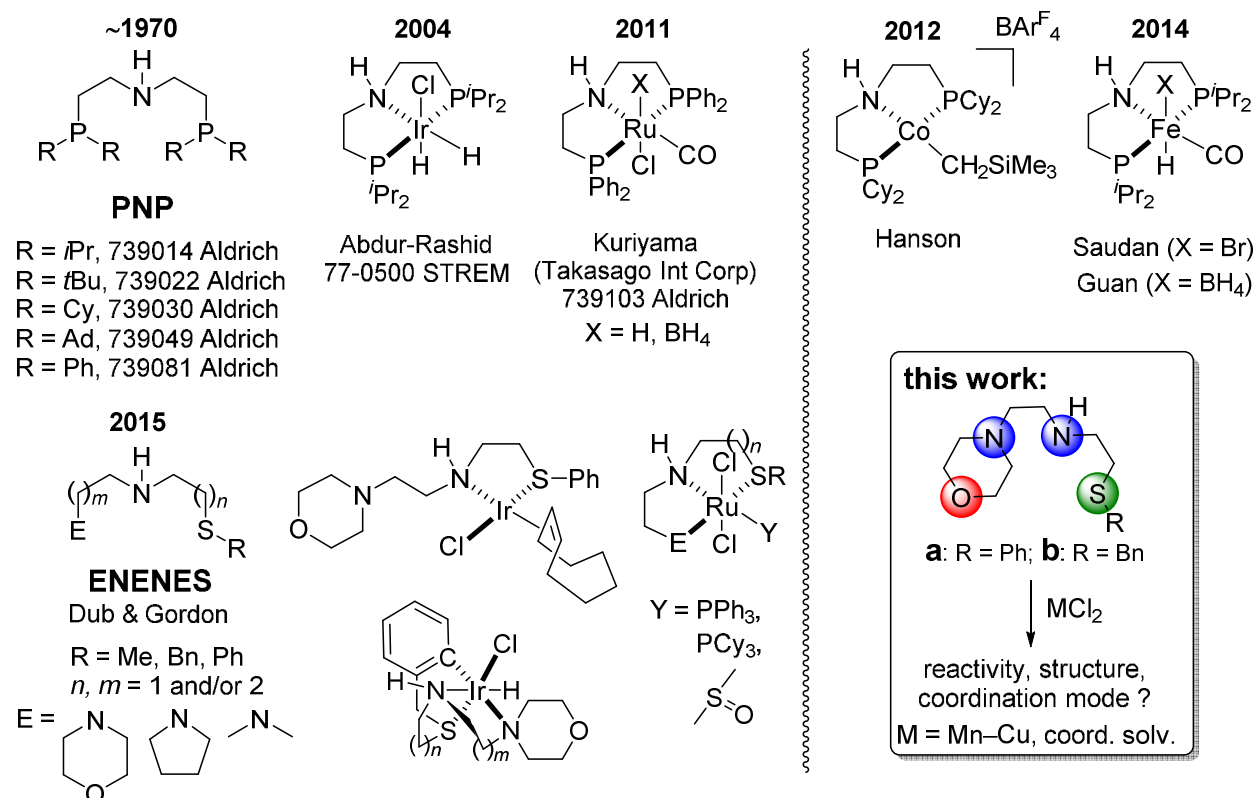


**Chart 1.**

Over the last few years, second and third row transition-metal complexes of Ru,<sup>6</sup> Os,<sup>6ad</sup> Ir<sup>1c, 5f, 6a, 6b, 6r, 6ac, 7</sup> as well as Mo<sup>8</sup> and W<sup>8</sup> supported by these ligands have been applied as (pre)catalysts in numerous homogeneous catalytic transformations. For example, the Ir complex [Ir<sup>III</sup>ClH<sub>2</sub>{(*i*Pr<sub>2</sub>PC<sub>2</sub>H<sub>4</sub>)<sub>2</sub>NH}] (Chart 1) originally developed by Abdur-Rashid for the transfer hydrogenation of ketones and imines,<sup>7i, 7k</sup> has been recently applied in the hydrogenation of ketones and aldehydes,<sup>7g, 7h</sup> CO<sub>2</sub> hydrogenation<sup>7d</sup> and electroreduction,<sup>7a</sup> ester hydrogenation,<sup>7b</sup> solvolysis of ammonia borane,<sup>7e</sup> amination of alcohols,<sup>7c, 7f</sup> hydrogen production from biomass-derived chemicals<sup>6a, 6b, 6r</sup> etc. The Ru complex [Ru<sup>II</sup>XH(CO){(Ph<sub>2</sub>PC<sub>2</sub>H<sub>4</sub>)<sub>2</sub>NH}] (Chart 1) originally developed by Kuriyama (Takasago Int. Corp.) for ester hydrogenation,<sup>6ab, 6ac</sup> was recently applied in homogeneous hydrogenations of other esters,<sup>6i, 6j, 6l, 6u-x</sup> CO<sub>2</sub>,<sup>6d, 6e</sup> carbonates,<sup>6aa</sup> nitriles,<sup>6g</sup> transfer hydrogenation of organic formates and cyclic carbonates,<sup>6k</sup>

various (acceptorless) dehydrogenations,<sup>6m, 6s, 6z, 6ad, 6ae</sup> selective  $\alpha$ - and  $\alpha,\beta$ -deuteration of alcohols,<sup>6c</sup> dehydrogenation<sup>6t, 6af-ah</sup> of ammonia or amine boranes, domino-synthesis of indoles,<sup>6n</sup> hydrogen production from biomass-derived chemicals,<sup>6a, 6b, 6r</sup> synthesis of substituted  $\gamma$ -lactones,<sup>6f</sup> synthesis of amides from esters and amines,<sup>6h</sup> diastereoselective amination<sup>6p</sup> etc.

Success in catalysis science relies on the development of new and novel ligands. Recently, we introduced “ENENES”,<sup>9,10</sup> a new family of NNS ligands containing an N–H functionality of general formula  $E(\text{CH}_2)_m\text{NH}(\text{CH}_2)_n\text{SR}$ , where E is selected from  $-\text{NC}_4\text{H}_8\text{O}$ ,  $-\text{NC}_4\text{H}_8$ ,  $-\text{N}(\text{CH}_3)_2$ ,  $m$  and  $n = 2$  and/or 3; R = Ph, Bn, Me (Chart 1). On the contrary to solid PNP-ligands bearing oxygen-sensitive P-atoms, liquid ENENES ligands are air-stable and can be easily accessed in multigram quantities in a variety of forms, since a range of cheap building blocks for their preparations are commercially available. Although sulfur has a tendency to poison transition-metal catalysts,<sup>11</sup> coordination of ENENES to Ru and Ir resulted in practical catalysts for the hydrogenation of ketones and fluorinated esters at ambient temperatures (for selected examples, see Chart 1).<sup>9,10</sup>

It is generally considered that if the reactions can be catalyzed by less-expensive metals, these processes maybe more industrially important.<sup>12</sup> The replacement of precious-metal catalysts with cheap and abundant (first row transition) metals was suggested,<sup>13</sup> and a variety of Cr,<sup>14</sup> Fe,<sup>6q, 15</sup> Co,<sup>16</sup> and Ni<sup>17</sup> (pre)catalysts supported by PNP were subsequently synthesized over the last few years. For example, Hanson and co-workers<sup>16b-e</sup> extensively modified the original Fryzuk  $[\text{Co}(\text{N}(\text{SiMe}_2\text{CH}_2\text{PPh}_2)_2)(\text{CH}_2\text{SiMe}_3)]$  complex<sup>18</sup> with  $\text{Cy}_2\text{P}(\text{CH}_2)_2\text{NH}(\text{CH}_2)_2\text{PCy}_2$  ligand and  $\text{HBAr}^{\text{F}}_4 \cdot 2\text{Et}_2\text{O}$  to find an active (pre)catalyst for hydrogenation/dehydrogenation reactions (Chart 1). Saudan<sup>15d</sup> and Guan<sup>15c</sup> modified the original Takasago’s Ru-MACHO complex to find a precatalyst for ester hydrogenation (Chart 1). Despite the growing popularity of first transition row element in homogeneous catalysis,<sup>19</sup> there are unfortunately three inherent problems associated with their use: 1) the activity expressed in turnover numbers and frequencies with first-row metals is barely catalytic (*cf.* Ru, Rh and Ir); 2) under such conditions, the price of the ligands themselves may become determining; 3) their complexes are usually air- and moisture-sensitive in the solid state (*cf.* Ru and Ir). Therefore, it is unlikely these pre(catalysts) will act as substitutes in powerful catalysis based on precious metals in the near future. Nevertheless, the exploration of coordination chemistry of novel ligands with first-transition row elements is of fundamental chemical interest.

Herein, we report reactions of two variants of ENENES, ligands **a** and **b** as shown in Chart 1, with first-row  $\text{MCl}_2$  precursors (M = Mn, Fe, Co, Ni and Cu) in coordinating solvents (MeCN, EtOH). The purpose of this work is to understand the reactivity of the above mentioned ligands with respect to selected metal precursors and to identify the resultant coordination mode depending on the basicity of the sulfur atom and the identity of a metal, via product isolation and crystallographical characterization. PNP ligands or their deprotonated counterparts usually coordinate to transition elements (other examples: Ru,<sup>20</sup> Fe,<sup>21</sup> Ir,<sup>22</sup> Pd,<sup>23</sup> Rh,<sup>24</sup> Re,<sup>25</sup> Co,<sup>26</sup>  $\text{V}^{5d}$ ) or actinides<sup>27</sup> via a  $\kappa^3[\text{N},\text{N}',\text{S}]$  coordination mode and typically in a *mer*-fashion. On the contrary, for the unsymmetrical ENENES systems, four different motifs,  $\kappa^2[\text{N},\text{N}']$ ,  $\kappa^2[\text{N}',\text{S}]$ ,  $\kappa^3[\text{N},\text{N}',\text{S}]$  and  $\kappa^4[\text{N},\text{N}',\text{S},\text{C}]$  were identified in reactions with suitable Ru or Ir precursors (for selected examples, see Chart 1).<sup>9,10</sup> Among various ENENES ligands, **a** and **b** were chosen because they contain a

morpholine moiety. Although polydentate ligands usually coordinate via only the nitrogen atom of such a moiety, a few reports (Chart 2)<sup>28</sup> have demonstrated the possibility of *N,O*-coordination in which coordination through the oxygen atom is hemilabile.

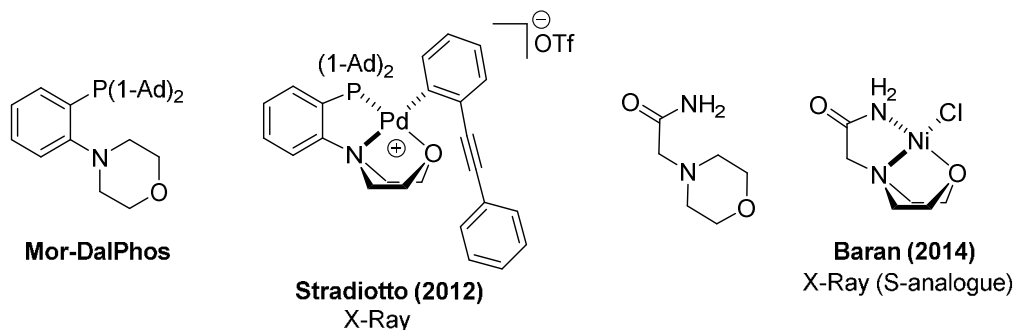


Chart 2.

**Experimental.** All complexes were prepared in an MBraun glovebox under an argon atmosphere. Acetonitrile (anhydrous, 99.8%, Sigma Aldrich), diethyl ether (anhydrous,  $\geq 99.7\%$ , Sigma Aldrich), absolute ethanol ( $\geq 99.5\%$ , Sigma Aldrich),  $MnCl_2$  ( $\geq 99\%$ , Sigma Aldrich),  $FeCl_2$  (98%, Sigma Aldrich),  $CoCl_2$  (97%, Acros Organics),  $NiCl_2$  (98%, Acros Organics),  $CuCl_2$  ( $\geq 99.995\%$ , Sigma Aldrich) were used as received. Elemental Analysis was performed by Midwest Microlab, LLC (Indianapolis, IN 46250) in air or under inert gas (argon or nitrogen), respectively.  $^1H$  NMR experiments were carried out using a Bruker AV400 MHz spectrometer in  $CDCl_3$  at room temperature. Complexes **2** and **6** are highly soluble in  $CDCl_3$ , while suspensions of complexes **1**, **3**, **4**, **5** and **7** were filtered through a Whatman syringe filter before recording spectra. The spectra are consistent with a high-spin formulation of complexes, see SI, Figures S1–S7. For example **2**, **3** and **4** exhibit broad resonances in the range from 260 to  $-60$  ppm ( $\delta$ ). The range narrows for Ni and Cu-complexes from 20 to  $-10$  ppm ( $\delta$ ), but resonances are still broad. The magnetic susceptibility measurements (Gouy balance, Sherwood Scientific, rt) performed with diamagnetic correction<sup>29</sup> confirm that these complexes are paramagnetic and high-spin, Table 1. A molecular weight corresponding to  $MnCl_2$ :a complex (392.24) was employed for **1**, consistent with elemental analysis data.

Table 1. Magnetic susceptibility measurements for complexes **1–7** in the solid state.<sup>a</sup>

Complex	M	$\mu_{eff}/\mu_B$ (T, °C)	$\mu_{calc}^b/\mu_B$	n.u.e. <sup>c</sup>	$\Delta\mu_{eff}^d/\mu_B$
<b>1</b>	Mn	6.9 (21)	5.9	5	5.7–6.1
<b>2</b>	Fe	5.5 (21)	4.9	4	5.1–5.7
<b>3</b>	Co	5.1 (21)	3.9	3	4.3–5.2
<b>4</b>	Co	4.4 (25)	3.9	3	4.3–5.2
<b>5</b>	Ni	3.6 (25)	2.8	2	2.8–3.5
<b>6</b>	Cu	2.1 (25)	1.7	1	1.7–2.2
<b>7</b>	Cu	1.9 (25)	1.7	1	1.7–2.2

<sup>a</sup> $\mu_{eff}$  = effective magnetic moment given in units of Bohr magnetons ( $\mu_B$ ). <sup>b</sup>Calculated for  $M^{2+}$  under standard conditions (spin-only value). <sup>c</sup>n.u.e. = number of unpaired electrons used for the calculations. <sup>d</sup> $\Delta\mu_{eff}$  range of typically found values under standard conditions.<sup>30</sup>

**Synthesis.** [ $\text{Mn}(\kappa^2[\text{N},\text{N}']\text{-a})\text{Cl}_2$ ] (**1**). To a pink suspension of  $\text{MnCl}_2$  (0.745 mmol, 94 mg) in MeCN (1 ml) was added a solution of **a** (0.745 mmol, 198 mg) in MeCN (3 ml) with stirring. Within 1–2 min, a white precipitate started to form. After 24 h, the precipitate was filtered, washed with MeCN (3 × 2 ml), diethyl ether (3 × 4 ml) and vacuum dried overnight. Yield: 220 mg (75 %), as a white powder. The compound is sparingly soluble in dichloromethane, THF, ethanol and acetonitrile. It dissolves immediately in water in air whereupon the obtained transparent solution slowly produces a yellowish precipitate, likely due to decomposition. Elem. Anal.: Calcd for  $\text{C}_{14}\text{H}_{22}\text{Cl}_2\text{MnN}_2\text{OS}$  (392.24): C, 42.87; H, 5.65; N, 7.14%; Found (under nitrogen): C, 42.06; H, 5.34; N, 6.92%.

**Crystals of** [ $\text{Mn}_4\text{Cl}_2(\mu_2\text{-Cl})_4(\mu_3\text{-Cl})_2(\kappa^2[\text{N},\text{N}']\text{-a})_4$ ] (**1'**). In a separate experiment, to a pink suspension of  $\text{MnCl}_2$  (0.745 mmol, 94 mg) in MeCN (1 ml) was added a solution of **a** (0.745 mmol, 198 mg) in MeCN (3 ml) with stirring. Within 1–2 min, a white precipitate started to form. After 2 h, the precipitate was filtered and the mother liquor was layered with diethyl ether. In ~3 months, transparent crystals formed that were characterized by X-Ray Diffraction Analysis.

[ $\text{Fe}(\kappa^2[\text{N},\text{N}']\text{-a})\text{Cl}_2$ ] (**2**). To a yellowish suspension of  $\text{FeCl}_2$  (0.745 mmol, 94 mg) in MeCN (1 ml) was added a solution of **a** (0.745 mmol, 198 mg) in MeCN (3 ml). The initial suspension slowly transformed into a light-green solution (ca. 1 h). After 2 h, the solution was filtered through a Whatman syringe filter (PTFE membrane, pore size 0.45  $\mu\text{m}$ ), concentrated to ~ 2 ml and layered with diethyl ether (~ 21 ml). Large light-green-blue block-like crystals were obtained overnight. Decantation of the mother liquor after 5 days and pumping to dryness afforded 223 mg of the compound (76 %). Elem. Anal.: Calcd for  $\text{C}_{14}\text{H}_{22}\text{Cl}_2\text{FeN}_2\text{OS}$  (393.15): C, 42.77; H, 5.64; N, 7.13%; Found (under nitrogen): C, 42.12; H, 5.45; N, 6.78%.

**Alternative work-up for 2.** After filtering the solution through a Whatman syringe filter as described above, the solvent was evaporated and the obtained residue was stirred with diethyl ether (7 ml) – pentane (7 ml) mixture to afford a white precipitate (overnight). The precipitate was collected, washed with diethyl ether (3 × 5 ml) and vacuum dried overnight. Yield: 215 mg (73 %), white powder. The paramagnetic material is oxygen-sensitive in both the solid state and (immediately) in solution. Elem. Anal.: Calcd for  $\text{C}_{14}\text{H}_{22}\text{Cl}_2\text{FeN}_2\text{OS}$  (393.15): C, 42.77; H, 5.64; N, 7.13%. Found (under argon): C, 42.59; H, 5.69; N, 7.01%.

[ $\text{Co}(\kappa^2[\text{N},\text{N}']\text{-a})\text{Cl}_2$ ] (**3**). To a blue suspension of  $\text{CoCl}_2$  (0.745 mmol, 97 mg) in MeCN (1 ml) was added a solution of **a** (0.745 mmol, 198 mg) in MeCN (3 ml). The obtained solution was stirred for 2 h, filtered through a Whatman syringe filter (PTFE membrane, pore size 0.45  $\mu\text{m}$ ), concentrated to ~ 2 ml and layered with diethyl ether (~ 21 ml). Blue crystals were obtained overnight. Decantation of the mother liquor after 5 days and pumping to dryness afforded 236 mg of the product (80 %). The compound is visually air- and moisture-stable, at least in the solid state, *i.e.*, as judged by maintenance of the color. Elem. Anal.: Calcd for  $\text{C}_{14}\text{H}_{22}\text{Cl}_2\text{CoN}_2\text{OS}$  (396.24): C, 42.44; H, 5.60; N, 7.07%; Found (in air): C, 42.27; H, 5.63; N, 7.08%.

**[Co( $\kappa^3$ [N,N',S]-b)Cl<sub>2</sub>] (4).** To a blue suspension of CoCl<sub>2</sub> (0.745 mmol, 97 mg) in MeCN (1 ml) was added a solution of **b** (0.745 mmol, 209 mg) in MeCN (3 ml). To the obtained mixture was added additionally MeCN (3 ml) for homogenization. The thus obtained blue solution was stirred for 2 h, concentrated to ~ half of the volume and layered with diethyl ether (~ 17 ml). Light-blue crystals were obtained overnight. Decantation of the mother liquor and pumping to dryness afforded 186 mg of the product (61 %). The compound is visually air- and moisture-stable at least in the solid state, *i.e.*, as judged by maintenance of the color. Elem. Anal.: Calcd for C<sub>15</sub>H<sub>24</sub>Cl<sub>2</sub>CoN<sub>2</sub>OS (410.26): C, 43.91; H, 5.90; N, 6.83%; Found (in air): C, 44.21; H, 5.92; N, 6.80%.

**trans-[Ni( $\kappa^3$ [N,N',S]-b)(EtOH)Cl<sub>2</sub>] (5).** A mixture of NiCl<sub>2</sub> (0.278 mmol, 36 mg) and **b** (0.278 mmol, 79 mg) in anhydrous EtOH (4 ml) was stirred in a Kontes pressure tube at 90 °C. After 44 h, the tube was cooled at -20°C for 1 h and the obtained greenish precipitate was collected on a filter frit, washed with EtOH (3 × 2 ml), then Et<sub>2</sub>O (3 × 4 ml) and dried under vacuum overnight. 77 mg of a greenish powder was recovered (61 %). Elem. Anal.: Calcd for C<sub>17</sub>H<sub>30</sub>Cl<sub>2</sub>NiN<sub>2</sub>O<sub>2</sub>S (456.09): C, 44.77; H, 6.63; N, 6.14%; Found (under nitrogen): C, 45.03; H, 6.50; N, 6.06%.

**[Cu( $\kappa^3$ [N,N',S]-a)Cl<sub>2</sub>] (6).** To a brown suspension of CuCl<sub>2</sub> (0.745 mmol, 100 mg) in MeCN (1 ml) was added a solution of **a** (0.745 mmol, 198 mg) in MeCN (3 ml). An immediate change in color to green was observed. The obtained solution was stirred for 4 h, filtered and the solvent evaporated under vacuum. To the obtained oily residue was added pentane (10 ml), and the mixture was stirred overnight to afford a green precipitate, that was collected, washed with pentane and dried under vacuum overnight. Yield: 272 mg (91%) of a visually air- and moisture-stable green solid, *i.e.*, as judged by maintenance of the color. Elem. Anal.: Calcd for C<sub>14</sub>H<sub>22</sub>Cl<sub>2</sub>CuN<sub>2</sub>OS (400.85): C, 41.95; H, 5.53; N, 6.99%; Found (in air): C, 41.88; H, 5.53; N, 6.84%.

**[Cu( $\kappa^3$ [N,N',S]-b)Cl<sub>2</sub>] (7).** To a brown suspension of CuCl<sub>2</sub> (0.684 mmol, 92 mg) in MeCN (2 ml) was added a solution of **b** (0.684 mmol, 192 mg) in MeCN (6 ml). An immediate change of color to green was observed. The obtained suspension was stirred for 4 h, the precipitate was filtered washed with diethyl ether (3 × 5 ml) and dried under vacuum overnight. Yield: 224 mg (79%) of a visually air- and moisture-stable sea-green solid, *i.e.*, as judged by maintenance of the color. Elem. Anal.: Calcd for C<sub>15</sub>H<sub>24</sub>Cl<sub>2</sub>CuN<sub>2</sub>OS (414.88): C, 43.43; H, 5.83; N, 6.75%; Found (in air): C, 42.83; H, 5.49; N, 6.58%.

**X-Ray Diffraction Studies.** Data for complexes **1'**, **2**, **3**, **5** and **7**·½hexane were collected on a Bruker D8 diffractometer, with an APEX II CCD detector. The crystals were cooled to an appropriate temperature as shown in Table 2 using a Bruker Kryoflex liquid nitrogen cryostat. Data for complex **4** were collected on a Bruker D8 Quest diffractometer, with CMOS detector in shutterless mode. The crystal was cooled to 100 K employing an Oxford Cryostream liquid nitrogen cryostat. The crystal quality did not allow satisfactory data refinement for **4**, however, the structural data is sufficient to establish the chemical connectivity and molecular geometry as shown in Figure 4, see SI for more details. All the data collections employed graphite

monochromatized MoK $\alpha$  ( $\lambda = 0.71073 \text{ \AA}$ ) radiation. The structure of 7·½hexane had disordered lattice solvent molecules, which were treated with Platon/Squeeze. Cell indexing, data collection, integration, structure solution, and refinement (full-matrix least-squares on  $F^2$ ) were performed using Bruker and Shelxtl software. Details of crystal and data collection parameters are summarized in Table 2. Additional details are included in the supplementary material.

Table 2. X-Ray Crystallographic Data for Complexes **1'**, **2**, **3**, **5**, and 7·½hexane.

	<b>1'</b>	<b>2</b>	<b>3</b>	<b>5</b>	7·½hexane
Empirical formula	C <sub>56</sub> H <sub>88</sub> Cl <sub>8</sub> Mn <sub>4</sub> N <sub>8</sub> O <sub>4</sub> S <sub>4</sub>	C <sub>14</sub> H <sub>22</sub> Cl <sub>2</sub> FeN <sub>2</sub> OS	C <sub>14</sub> H <sub>22</sub> Cl <sub>2</sub> CoN <sub>2</sub> OS	C <sub>17</sub> H <sub>30</sub> Cl <sub>2</sub> N <sub>2</sub> NiO <sub>2</sub> S	C <sub>18</sub> H <sub>31</sub> Cl <sub>2</sub> CuN <sub>2</sub> OS
Formula weight	1568.94	393.15	396.23	456.10	457.95
Temperature/K	140(1)	100(2)	120(1)	140(1)	140(1)
Crystal system	monoclinic	monoclinic	triclinic	triclinic	orthorhombic
Space group	P 2 <sub>1</sub> /n	P 2 <sub>1</sub> /n	P -1	P -1	P bca
a/Å	12.171(3)	7.0525(6)	7.127(2)	6.484(3)	13.2833(17)
b/Å	11.594(3)	21.2477(19)	11.307(4)	8.921(4)	11.5401(15)
c/Å	24.657(5)	23.0147(17)	11.422(4)	19.032(9)	26.694(4)
$\alpha$ /degree	90	90	98.291(3)	98.492(7)	90
$\beta$ /degree	100.927(2)	90.269(4)	107.707(3)	98.646(6)	90
$\gamma$ /degree	90	90	94.031(4)	106.341(6)	90
Volume/Å <sup>3</sup>	3416.3(13)	3448.7(5)	861.3(5)	1023.2(8)	4091.9(9)
Z	2	8	2	2	8
D <sub>calc</sub> /Mg·m <sup>-3</sup>	1.525	1.514	1.528	1.480	1.487
Absorption coefficient/mm <sup>-1</sup>	1.207	1.305	1.427	1.325	1.440
F(000)	1624	1632	410	480	1920
Crystal size/mm <sup>3</sup>	0.20 × 0.08 × 0.06	0.29 × 0.26 × 0.22	0.30 × 0.30 × 0.10	0.20 × 0.08 × 0.02	0.30 × 0.26 × 0.02
Theta range for data collection/degree	1.68 to 26.33	1.30 to 25.68	1.90 to 28.58	2.21 to 28.46	2.16 to 25.77
Index ranges	-15 ≤ h ≤ 15 -14 ≤ k ≤ 14 -30 ≤ l ≤ 30	-8 ≤ h ≤ 8 -25 ≤ k ≤ 25 -28 ≤ l ≤ 28	-9 ≤ h ≤ 9 -14 ≤ k ≤ 15 -14 ≤ l ≤ 14	-8 ≤ h ≤ 7 -11 ≤ k ≤ 11 -24 ≤ l ≤ 25	-16 ≤ h ≤ 16 -14 ≤ k ≤ 14 -32 ≤ l ≤ 32
Reflections collected	34216	59050	9966	5970	38636
Independent reflections	6901 [R(int) = 0.0726]	6557 [R(int) = 0.0761]	4033 [R(int) = 0.0137]	4198 [R(int) = 0.0287]	3921 [R(int) = 0.0639]
Completeness to theta = 25.00°/%	99.9	100.0	99.7	91.9	100.0
Max. and min. transmission	0.9311 and 0.7943	0.7578 and 0.7050	0.8705 and 0.6742	0.9740 and 0.7776	0.9718 and 0.6719
Data/restraints /parameters	6901/0/379	6557/0/385	4033/0/190	4198/0/230	3921/0/199
Goodness-of-fit on F <sup>2</sup>	1.102	1.163	1.060	1.096	1.084
Final R indices [I > 2σ(I)]	R1 = 0.0402, wR2 = 0.0996	R1 = 0.0332, wR2 = 0.0700	R1 = 0.0358, wR2 = 0.0838	R1 = 0.0655, wR2 = 0.1311	R1 = 0.0292, wR2 = 0.0633
R indices (all data)	R1 = 0.0518, wR2 = 0.1061	R1 = 0.0504, wR2 = 0.0762	R1 = 0.0381, wR2 = 0.0854	R1 = 0.1171, wR2 = 0.1539	R1 = 0.0424, wR2 = 0.0665
Largest diff. peak and hole/e.Å <sup>-3</sup>	0.593 and -0.640	0.522 and -0.387	1.775 and -0.887	0.649 and -0.697	0.365 and -0.315

**Computational Studies.** Computational analysis was carried out at the DFT<sup>31</sup>/ωB97X-D<sup>32</sup>/ECP\_ECP10MDF(Co)<sup>33</sup>/6-311++G\*\* (C,H,N,O,S,Cl) level of theory with an increased integral accuracy ( $1 \times 10^{-11}$ ) using code Gaussian 09 (rev. D01).<sup>34</sup> The computations were performed in the gas-phase for Co-complexes with a multiplicity of 4 corresponding to  $S = 3/2$ . An example of an input file is provided in SI. All the wavefunctions were tested for stability for each optimized structure. Molecular graphics were performed with the UCSF Chimera package.<sup>35</sup>

**Results and Discussion.** The reaction of pink MnCl<sub>2</sub> with an equimolar amount of ligand **a** in acetonitrile resulted in the formation of a white solid immediately in 1–2 min after mixing the



reagents and stirring was applied. The heterogeneous reaction was not completed within at least 1 h as evidenced by visual observation of pink solid material still present in the reaction mixture. In 2–6 hours, the reaction mixture resulted in a white suspension, but the elemental analysis of the separated white powder was not satisfactory and was not well reproducible, being far from a 1:1 stoichiometry. On the other hand, X-Ray diffraction analysis performed on the colorless crystals obtained from a mother liquor separated in 2 h from the white powder identified a tetranuclear  $C_i$ -symmetric chlorido-bridged manganese(II) cluster  $[\text{Mn}_4\text{Cl}_2(\mu_2\text{-Cl})_4(\mu_3\text{-Cl})_2(\kappa^2[N,N']\text{-a})_4]$  (**1'**) as shown in Figure 1, which is, likely an intermediate or a by-product that is intercepted in the reaction mixture of an incomplete reaction as shown in Scheme 1.

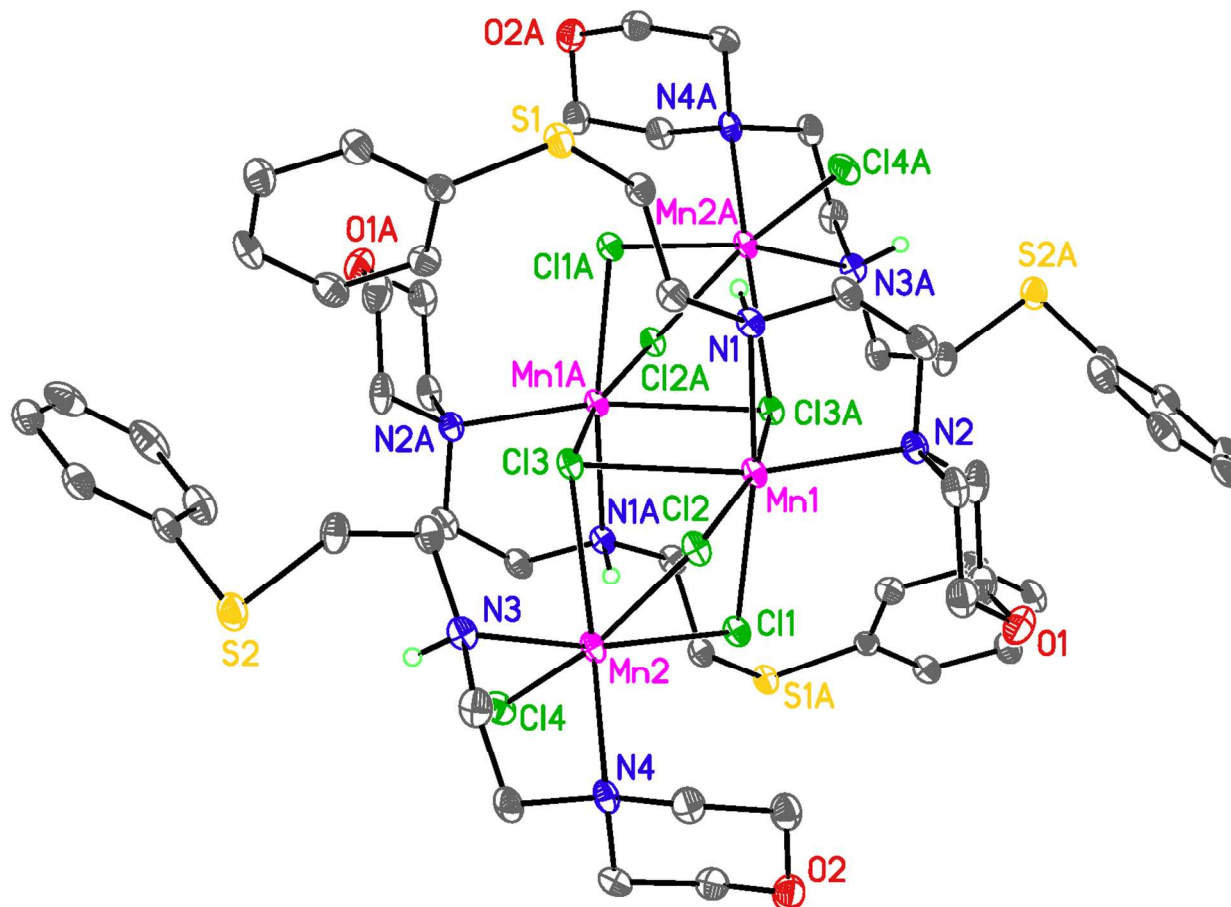
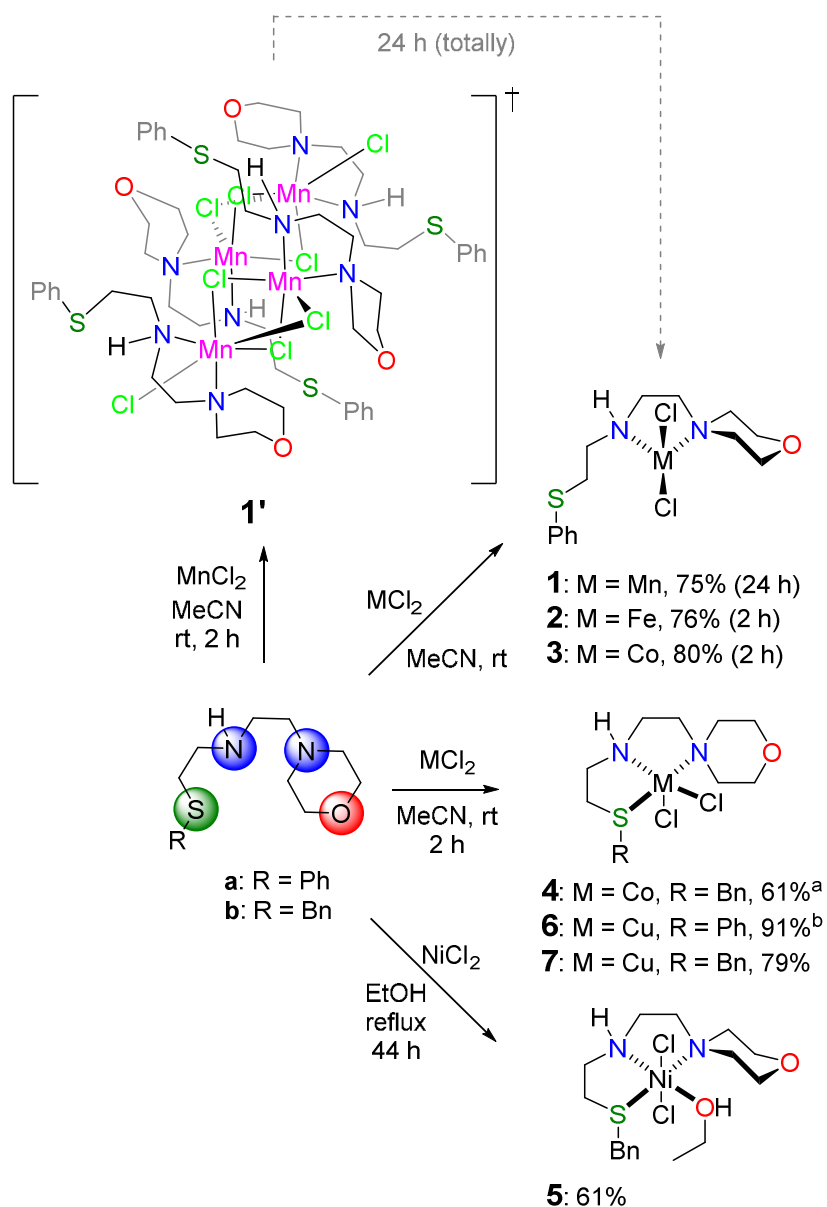


**Figure 1.** X-Ray molecular structure for Mn cluster-complex **1'** (50% level of thermal ellipsoids). H-atoms (except NH) are omitted for clarity. Selected bond distances (Å): Mn1–Mn2, 3.3997(8); Mn1–Mn1a, 3.867(9); Mn1–N1, 2.247(2); Mn1–N2, 2.333(2); Mn1–Cl2, 2.5143(9); Mn1–Cl1, 2.5245(8); Mn1–Cl3, 2.7116(8); Mn1–Cl3A, 2.5546(9); Mn2–N3, 2.269(2); Mn2–N4, 2.359(2); Mn2–Cl4, 2.4143(9). Symm. a: 1-x, 2-y, 2-z.



**Scheme 1.** Reactions of  $MCl_2$  ( $M = Mn, Fe, Co, Ni$  and  $Cu$ ) with ligands **a–b** in coordinating solvents. †Tetra-nuclear  $C_1$ -symmetric chlorido-bridged manganese(II) cluster  $[Mn_4Cl_2(\mu_2-Cl)_4(\mu_3-Cl)_2(\kappa^2[N,N']-a)_4]$  (**1'**) obtained from a mother liquor of **1** was possibly intercepted in the reaction mixture as an intermediate or a by-product of the reaction between  $MnCl_2$  and ligand **a** in 2 h, see text. <sup>a</sup>Morpholine moiety adopts equatorial conformation mode (X-Ray). <sup>b</sup>Morpholine moiety adopts axial conformation mode (X-Ray).

Only after 24 h stirring, a white powder was obtained that gave reproducible elemental analysis corresponding to a 1:1 stoichiometry of  $MnCl_2:a$ . We suggest the identity of the material as  $[Mn(\kappa^2[N,N']-a)Cl_2]$  (**1**), obtained in 75% isolated yield as shown in Scheme 1. A  $\kappa^2[N,N']$  mode of coordination is suggested by X-Ray structural analysis for complex **1'** (as well as **2** and

**3**, see below), whereas its identity as a mononuclear  $Mn_1$  species rather than a tetranuclear  $Mn_4$  is suggested by a different X-Ray powder diffraction (XRD) pattern observed for **1** and predicted for **1'**, see Figure S8. The experimental magnetic susceptibility measurement for complex **1** is consistent with a paramagnetic, high-spin formulation, Table 1. The complex is sparingly soluble in organic solvents under argon but was immediately solubilized by water in air, where possible decomposition takes place. On the other hand, visually, the compound appears to be stable in air in the solid state, but seems to be highly hygroscopic.

On the contrary to  $MnCl_2$ , the reactions of  $MCl_2$  ( $M = Fe, Co$ ) with ligand **a** were homogeneous under the same conditions. Crystallizations afforded the paramagnetic, tetrahedral complexes  $[M(\kappa^2[N,N']-a)Cl_2]$ ,  $M = Fe$  (**2**),  $Co$  (**3**) isolated in 76% and 80% yield, respectively as shown in Scheme 1. Their composition and purity were confirmed by elemental analyses and their solid-state molecular structures were determined by single crystal X-Ray diffraction as shown in Figure 2 and Figure 3, respectively. In both cases and in a similar fashion to  $MnCl_2$ , ligand **a** binds in a bidentate  $\kappa^2[N,N']$  fashion via two  $N$ -atoms.

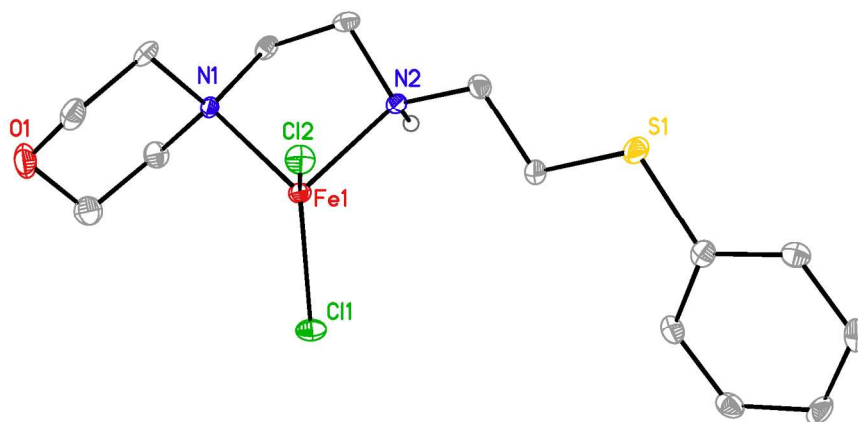


**Figure 2.** X-Ray molecular structure for Fe-complex **2** (50% level of thermal ellipsoids). H-atoms (except NH) are omitted for clarity. Selected bond distances ( $\text{\AA}$ ): Fe1–Cl1, 2.2401(7); Fe1–Cl2, 2.2456(7); Fe1–N1, 2.1689(19); Fe1–N2, 2.135(2). Selected angles ( $^\circ$ ): N1–Fe1–N2, 83.30(8); Cl1–Fe1–Cl2, 122.14(3).

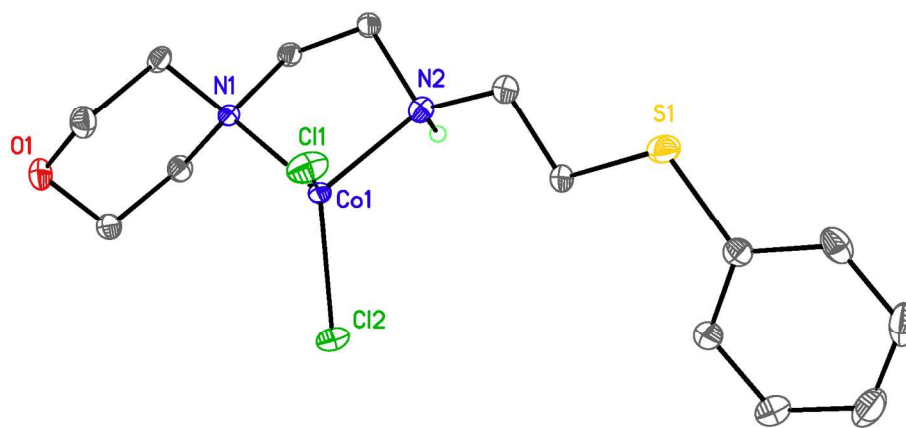


**Figure 3.** X-Ray molecular structure for Co-complex **3** (50% level of thermal ellipsoids). H-atoms (except NH) are omitted for clarity. Selected bond distances (Å): Co1–Cl1, 2.2227(8); Co1–Cl2, 2.2301(8); Co1–N1, 2.1005(19); Co1–N2, 2.069(2). Selected angles (°): N1–Co1–N2, 87.14(8); Cl1–Co1–Cl2, 112.77(3).

Selected stationary points of the gas-phase PES (Potential Energy Surface) for the system **a**–CoCl<sub>2</sub> with spin  $S = 3/2$  optimized at the DFT<sup>31</sup>/ωB97X-D<sup>32</sup>/ECP\_ECP10MDF(Co)<sup>33</sup>/6-311++G\*\*(C,H,N,O,S,Cl) level of theory are shown in Figure 4. The most stable structure **3A**, corresponds to a  $\kappa^2[N,N']$  coordination mode, just as observed in the solid state by X-Ray structural analysis. Structures **3E** and **3F** correspond to  $\kappa^2[S,N']$  bidentate and  $\kappa^4[O,N,N',S]$  tetradentate coordination modes and are significantly uphill in energy by 10.5 and 11.1 kcal·mol<sup>-1</sup> ( $\Delta G^\circ_{298K}$ ), respectively. On the other hand, there is a much smaller energy gap for structure **3B** corresponding to a tridentate  $\kappa^3[N,N',S]$  coordination mode ( $\Delta\Delta G^\circ_{298K} = 0.5$  kcal·mol<sup>-1</sup>). Structures **3C** and **3D** also correspond to the  $\kappa^3[N,N',S]$  coordination mode, but differ from **3B** either by the absolute configuration of the sulfur atom (**3D**), or by the conformational arrangement of the morpholine moiety (**3C**), being equatorial for **3B** and axial for **3C**, respectively. The energy difference between **3A** and **3B** suggests that fine-tuning of electronic density at the sulfur atom in the NNS ligand may favor a structure with a  $\kappa^3[N,N',S]$  coordination mode.

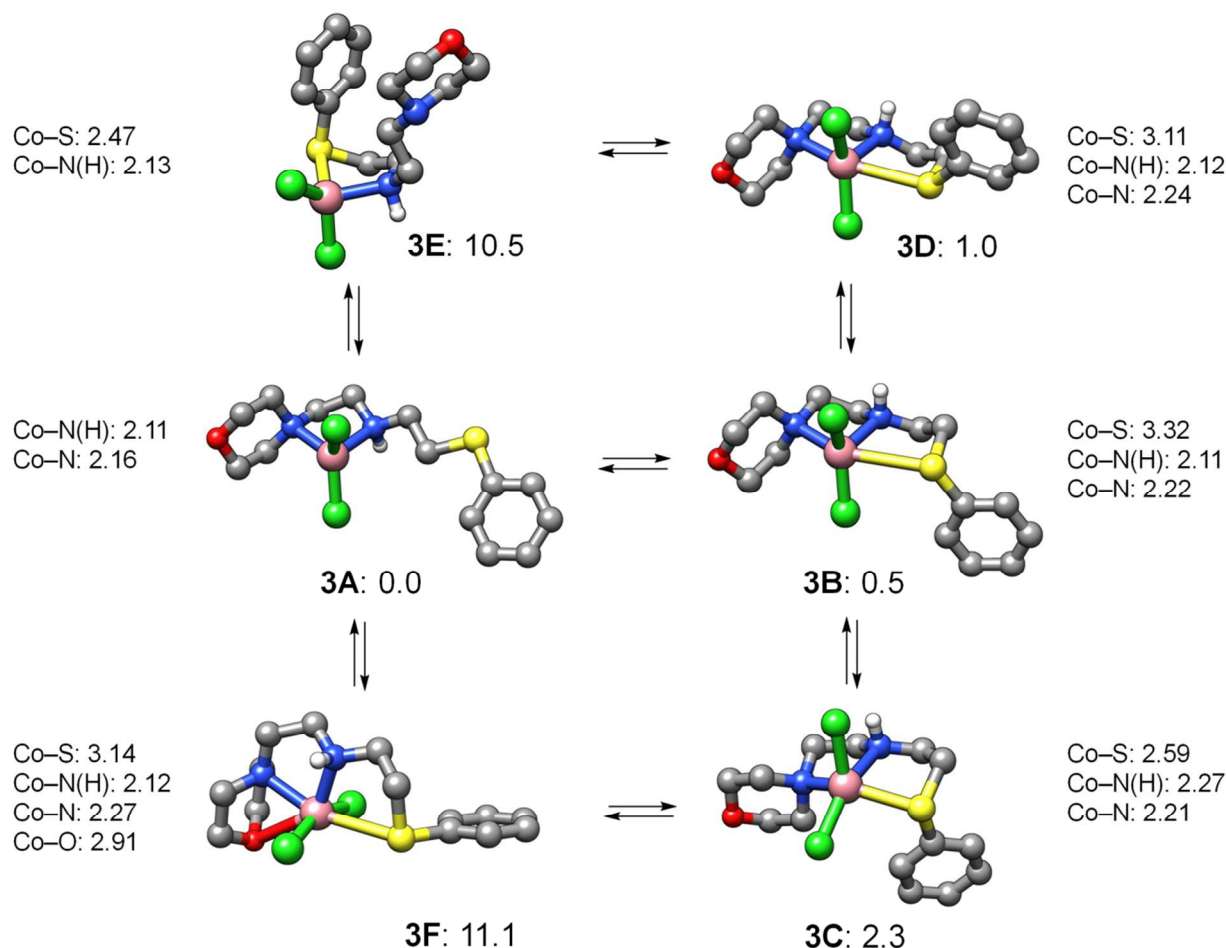


**Figure 4.** Selected stationary points of the PES for the system **a**-CoCl<sub>2</sub> with  $S = 3/2$ . Optimized at the DFT<sup>31</sup>/ $\omega$ B97X-D<sup>32</sup>/ECP\_ECP10MDF(Co)<sup>33</sup>/6-311++G\*\*(C,H,N,O,S,Cl) level of theory. Selected bond lengths are represented in angstroms (Å). The relative free energy  $G^\circ_{298\text{K}}$  values are given in kcal·mol<sup>-1</sup>. H-atoms (except NH) are omitted for clarity.

Indeed, when CoCl<sub>2</sub> was reacted with ligand **b** bearing a more basic sulfur atom under the same conditions as ligand **a**, a light-blue-colored  $\kappa^3[N,N',S]$  meridional tridentate complex, [Co( $\kappa^3[N,N',S]$ -**b**)Cl<sub>2</sub>] (**4**) was isolated in 61% isolated yield after the first crystallization. The composition and purity of **4**<sup>36</sup> was confirmed by elemental analysis, and its solid-state molecular structure was determined by X-Ray diffraction as shown in Scheme 1 and Figure 5, respectively. For comparison with more electron rich PNP ligands, their reactions with FeCl<sub>2</sub> or CoCl<sub>2</sub> afford tridentate  $\kappa^3[P,N,P]$  and pentacoordinate [M( $\kappa^3[P,N,P]$ -ligand)Cl<sub>2</sub>] (M = Fe,<sup>37</sup> Co<sup>5a, 5f, 16f, 16g</sup>) complexes, at least in the solid state.

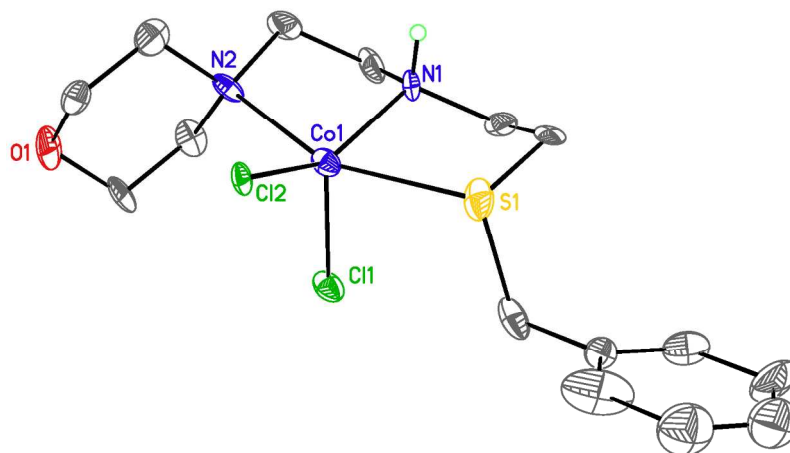


**Figure 5.** X-Ray molecular structure for Co-complex **4** (50% level of thermal ellipsoids). H-atoms (except NH) molecules are omitted for clarity. Selected bond distances (Å): Co1–Cl1, 2.292(3); Co1–Cl2, 2.294(3); Co1–N1, 2.042(9); Co1–N2, 2.325(10); Co1–S1, 2.599(3). Selected angles (°): N1–Co1–N2, 81.2(3); Cl1–Co1–Cl2, 112.72(12); N1–Co1–Cl1, 102.6(3); N1–Co1–Cl2, 143.7(3); N1–Co1–S1, 80.0(3).

Computations performed at the same level of theory for the system **b**–CoCl<sub>2</sub> with  $S = 3/2$  nicely predict the experimental result as shown in Figure 6. The most stable structure **4B** corresponds to the  $\kappa^3[N,N',S]$  coordination mode in which the morpholine moiety adopts equatorial arrangement.<sup>38</sup>

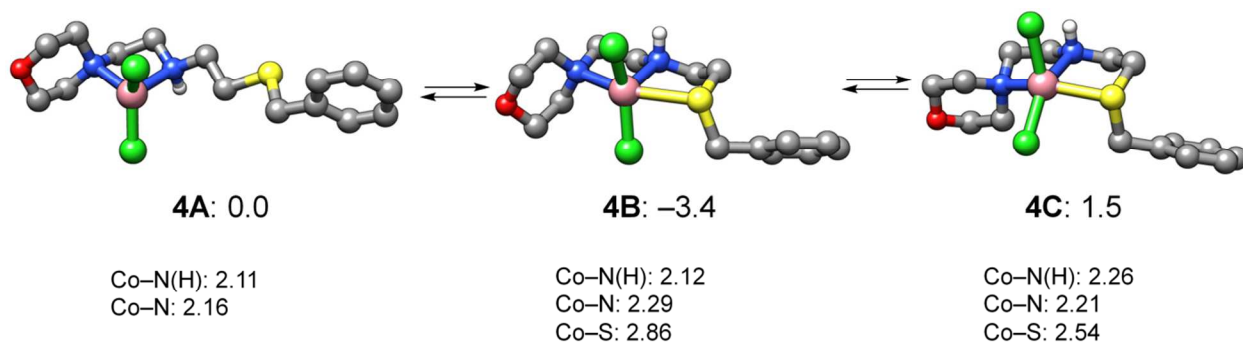


**Figure 6.** Selected stationary points of the PES for the system **b**–CoCl<sub>2</sub> with  $S = 3/2$ . Optimized at DFT<sup>31</sup>/ $\omega$ B97X-D<sup>32</sup>/ECP\_ECP10MDF(Co)<sup>33</sup>/6-311++G\*\*(C,H,N,O,S,Cl) level of theory. Selected bond lengths are presented in angstroms (Å). The relative free energy  $G^{\circ}_{298\text{K}}$  values are given in kcal·mol<sup>-1</sup>. H-atoms (except NH) are omitted for clarity.

No visible reaction occurred when yellow, acetonitrile insoluble  $\text{NiCl}_2$  was reacted with an equimolar amount of **a** or **b** after 5 days at room temperature. On the contrary, refluxing a 1:1 mixture of  $\text{NiCl}_2$  and **b** in ethanol for 44 h, afforded a green paramagnetic precipitate in 61% isolated yield, that has been identified as the well-defined complex *trans*- $[\text{Ni}(\kappa^3[\text{N},\text{N}',\text{S}]-\text{b})\text{Cl}_2(\text{EtOH})]$  (**5**), based on elemental and X-Ray structural analysis as shown in Scheme 1 and in Figure 7, respectively. In a similar fashion to complex **4**, ligand **b** binds to the metal in **5** in a tridentate meridional  $\kappa^3[\text{N},\text{N}',\text{S}]$  fashion via two nitrogen and a S–Bn moiety, respectively. In this case, an additional coordinated solvent molecule occupies the sixth metal coordination site in the position *trans* to the N(H) atom. The Ni–O bond length of 2.089(4) is comparable to those of 2.085(8) Å in  $[\text{NiCl}_2(\text{H}_2\text{O})_3(\text{C}_2\text{H}_5\text{OH})]$ .<sup>39</sup> For comparison with the PNP class of ligands, the available X-Ray structure of  $[\text{Ni}\{\text{NH}(\text{CH}_2\text{CH}_2\text{PPh}_2)_2\}\text{Cl}]\text{Cl}$ <sup>40</sup> consists of a discrete square planar  $[\text{M}(\text{PNP})\text{Cl}]^+$  cation and an uncoordinated chloride anion.

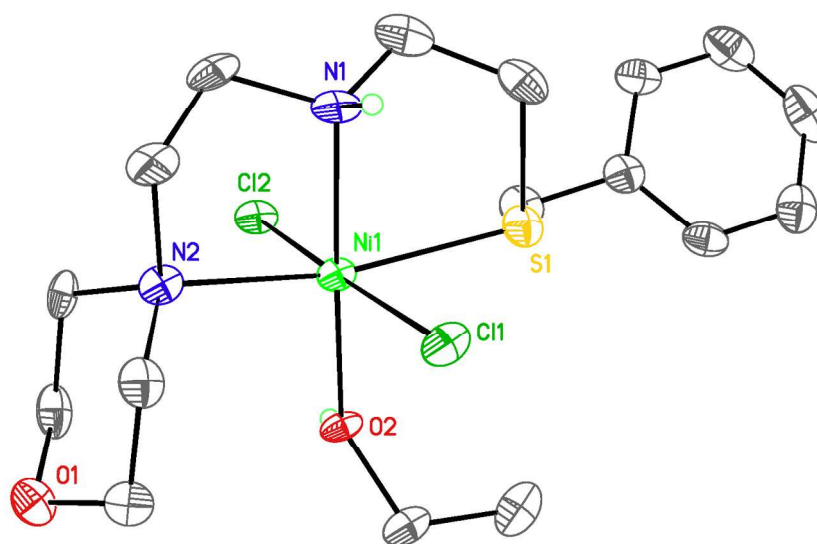


**Figure 7.** X-Ray molecular structure for Ni-complex **5** (50% level of thermal ellipsoids). H-atoms (except NH and OH) are omitted for clarity. Selected bond distances (Å): Ni1–Cl1, 2.4038(15); Ni1–Cl2, 2.4192(15); Ni1–N1, 2.054(4); Ni1–N2, 2.259(4); Ni1–S1, 2.4588(18); Ni1–O2, 2.089(4). Selected angles (°): N1–Ni1–O2, 173.38(15); N1–Ni1–N2, 82.72(16); Cl1–Ni1–Cl2, 174.78(5).

The room temperature reaction of brown  $\text{CuCl}_2$  with an equimolar amount of **a** or **b** in acetonitrile resulted in the formation of air- and moisture-stable green and sea green complexes  $[\text{Cu}(\kappa^3[\text{N},\text{N}',\text{S}]-\text{ligand})\text{Cl}_2]$ , ligand = **a** (**6**), **b** (**7**), in 91% and 79% isolated yield, respectively as shown in Scheme 1. These contain the NNS ligand bound in a tridentate fashion, as suggested by the green color typically attributed to a  $\sigma(\text{S}) \rightarrow d(\text{Cu})$  charge transfer.<sup>41</sup> The composition of these complexes was confirmed by elemental and X-Ray structural analysis for  $7 \cdot \frac{1}{2}$ hexane as shown in Figure 8. The structure of **7** is similar to copper(II) complexes bearing tridentate meridional NNS ligand derivatives of pyridine,<sup>41a, 42</sup> *i.e.* the Cu(II) atom possesses a five-coordinate, distorted

square-pyramidal geometry with a Cl1–Cu–Cl2 angle of  $104.74(2)^\circ$ . A notable difference is the shorter Cu–Cl2 bond length of  $2.4974(7) \text{ \AA}$  (*cf.*  $2.648\text{--}2.659$ )<sup>41a, 42</sup> for the copper axial chloride-atom bond lengths. It is also interesting to note that the morpholine moiety in **7** adopts an axial conformation, contrary to all complexes described herein in which equatorial coordination is observed. We remind the reader that these conformations are separated by  $\sim 1 \text{ kcal}\cdot\text{mol}^{-1}$  in a morpholine molecule.<sup>43</sup> Such an arrangement is likely responsible for the different structures observed for **7** versus **4** in the solid state which differ in the value of the N(H)–M–Cl2 angle (*cf.* also **3B** and **3C** in Figure 4).

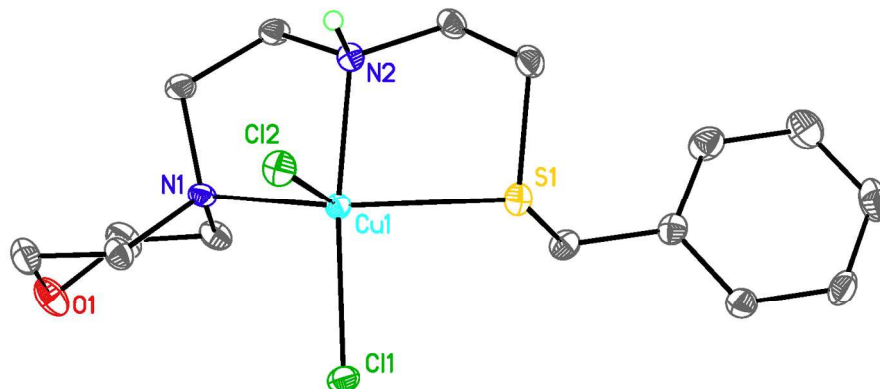


**Figure 8.** X-Ray molecular structure for Cu-complex **7**·½hexane (50% level of thermal ellipsoids). H-atoms (except NH) and solvent molecule are omitted for clarity. Selected bond distances ( $\text{\AA}$ ): Cu1–Cl1,  $2.2619(6)$ ; Cu1–Cl2,  $2.4974(7)$ ; Cu1–N1,  $2.0838(18)$ ; Cu1–N2,  $2.0135(18)$ ; Cu1–S1,  $2.3627(7)$ . Selected angles ( $^\circ$ ): N1–Cu1–S1,  $161.87(5)$ ; N1–Cu1–N2,  $85.39(7)$ ; Cl1–Cu1–Cl2,  $104.74(2)$ ; N2–Cu1–Cl2,  $90.27(5)$ ; N2–Cu1–Cl1,  $164.80(5)$ .

**Conclusions.** We have studied a series of reactions between potentially tetradenate ENENES ligands **a** and **b** and  $\text{MCl}_2$  compounds ( $\text{M} = \text{Mn, Fe, Co, Ni}$  and  $\text{Cu}$ ) in coordinating solvents is reported. Products were isolated and crystallographically characterized. It was observed that for the harder metal atoms ( $\text{Mn, Fe}$ ) less basic ligand **a** binds in a  $\kappa^2[\text{N},\text{N}']$ -fashion, whereas for the softer metals ( $\text{Ni, Cu}$ ), more basic ligand **b** (or **a** at least for  $\text{Cu}$ ) bind in a  $\kappa^3[\text{N},\text{N}',\text{S}]$ -fashion. For  $\text{Co}$  (intermediate in hardness),  $\kappa^2[\text{N},\text{N}']$  and  $\kappa^3[\text{N},\text{N}',\text{S}]$  coordination modes were identified in the reactions with **a** and **b**, respectively. DFT calculations can be used to predict the coordination mode. Coordination of the oxygen-atom within the 4-morpholinyl moiety of the ligand was not observed. A possible reason for this the too unfavorable thermodynamics,  $\sim 8 \text{ kcal}\cdot\text{mol}^{-1}$ ,<sup>43</sup> required with respect to a chair  $\rightarrow$  skew-boat rearrangement within this moiety.

**Electronic supplementary information (ESI) available:** Additional details for the X-Ray data,  $^1\text{H}$  NMR spectra for complexes, XRD for **1**, example of an input file, table of energy data, Cartesian coordinates for optimized structures. CCDC 1429177-1429181 for **1'**, **2**, **3**, **5** and **7**·½hexane. For ESI and crystallographic data in CIF or other electronic format see DOI: *to be filled by editorial staff*.



## ACKNOWLEDGEMENTS

PAD is recipient of a J. Robert Oppenheimer (JRO) Distinguished Postdoctoral Fellowship at LANL. We thank Drs Michael L. Neville and Tim Boyle (Sandia National Laboratories, Albuquerque, NM) for aiding with the X-Ray structure of complex **2** and are grateful for the use of the Bruker X-Ray diffractometer purchased via the National Science Foundation CRIF:MU award to Prof. Rick Kemp of the University of New Mexico (CHE04-43580). Computations were performed at the Center for Integrated Nanotechnologies, an Office of Science User Facility operated for the U.S. Department of Energy (DOE) Office of Science by Los Alamos National Laboratory (Contract DE-AC52-06NA25396) and Sandia National Laboratories (Contract DE-AC04-94AL85000).

## REFERENCES

- (a) P. C. J. Kamer and P. W. N. M. van Leeuwen, eds., *Phosphorus(III) Ligands in Homogeneous Catalysis: Design and Synthesis*, John Wiley & Sons Ltd., 2012; (b) Q.-L. Zhou, ed., *Privileged Chiral Ligands and Catalysts*, Wiley-VCH Verlag GmbH & Co. KGaA, 2011; (c) C. Mueller and D. Vogt, *Catal. Met. Complexes*, 2011, **37**, 151-181; (d) A. Grabulosa and Editor, *P-Stereogenic Ligands in Enantioselective Catalysis*, Royal Society of Chemistry Publishing, 2011.
- B. Zhao, Z. Han and K. Ding, *Angew. Chem., Int. Ed.*, 2013, **52**, 4744-4788.
- (a) S. Kuwata and T. Ikariya, *Chem. Commun.*, 2014, **50**, 14290-14300; (b) T. Ikariya and Y. Kayaki, *Pure Appl. Chem.*, 2014, **86**, 933-943; (c) P. A. Dub and T. Ikariya, *ACS Cat.*, 2012, **2**, 1718-1741; (d) T. Ikariya and M. Shibasaki, *Topics in Organometallic Chemistry: Bifunctional Molecular Catalysis*, Springer: New York, 2011; (e) T. Ikariya, *Bull. Chem. Soc. Jpn.*, 2011, **84**, 1-16; (f) T. Ikariya and I. D. Gridnev, *Top. Catal.*, 2010, **53**, 894-901; (g) T. Ikariya and I. D. Gridnev, *Chem. Rec.*, 2009, **9**, 106-123; (h) T. Ikariya and A. J. Blacker, *Acc. Chem. Res.*, 2007, **40**, 1300-1308; (i) T. Ikariya, K. Murata and R. Noyori, *Org. Biomol. Chem.*, 2006, **4**, 393-406; (j) K. Muñiz, *Angew. Chem., Int. Ed.*, 2005, **44**, 6622-6627; (k) R. Noyori, C. A. Sandoval, K. Muniz and T. Ohkuma, *Philos. Trans. R. Soc. A-Math. Phys. Eng. Sci.*, 2005, **363**, 901-912; (l) R. Noyori, M. Kitamura and T. Ohkuma, *Proc. Natl. Acad. Sci. U. S. A.*, 2004, **101**, 5356-5362; (m) R. Noyori, *Angew. Chem., Int. Ed.*, 2002, **41**, 2008-2022; (n) R. Noyori, M. Yamakawa and S. Hashiguchi, *J. Org. Chem.*, 2001, **66**, 7931-7944.
- (a) S. Schneider, J. Meiners and B. Askevold, *Eur. J. Inorg. Chem.*, 2012, **2012**, 412-429; (b) D. Amoroso, K. Abdur-Rashid, X. Chen, R. Guo, W. Jia and S. Lu, *Strem Chem.*, 2011, **25**, 4-26; (c) J. I. van der Vlugt and J. N. H. Reek, *Angew. Chem., Int. Ed.*, 2009, **48**, 8832-8846.
- (a) L. Sacconi and R. Morassi, *J. Chem. Soc. A*, 1968, 2997-3002; (b) M. E. Wilson, R. G. Nuzzo and G. M. Whitesides, *J. Am. Chem. Soc.*, 1978, **100**, 2269-2270; (c) R. G. Nuzzo, S. L. Haynie, M. E. Wilson and G. M. Whitesides, *J. Org. Chem.*, 1981, **46**, 2861-2867; (d) A. A. Danopoulos and P. G. Edwards, *Polyhedron*, 1989, **8**, 1339-1344; (e) A. A. Danopoulos, A. R. Wills and P. G. Edwards, *Polyhedron*, 1990, **9**, 2413-2418; (f) K. Abdur-Rashid, T. Graham, C.-W. Tsang, X. Chen, R. Guo, W. Jia, D. Amoroso and C. Sui-Seng, WO2008141439A1, 2008.
- (a) Y. Li, P. Sponholz, M. Nielsen, H. Junge and M. Beller, *ChemSusChem*, 2015, **8**, 804-808; (b) Y. Li, M. Nielsen, B. Li, P. H. Dixneuf, H. Junge and M. Beller, *Green Chemistry*, 2015, **17**, 193-198; (c) B. Chatterjee and C. Gunanathan, *Org. Lett.*, 2015, **17**, 4794-4797; (d) L. Zhang, Z. Han, X. Zhao, Z. Wang and K. Ding, *Angew. Chem., Int. Ed.*, 2015, **54**, 6186-6189; (e) N. M. Rezayee, C. A. Huff and M. S. Sanford, *J. Am. Chem. Soc.*, 2015, **137**, 1028-1031; (f) M. Pena-Lopez, H. Neumann and M. Beller, *Chem. Commun.*, 2015, **51**, 13082-13085; (g) J. Neumann, C.

- Bornschein, H. Jiao, K. Junge and M. Beller, *Eur. J. Org. Chem.*, 2015, **2015**, 5944-5948; (h) Q. Han, X. Xiong and S. Li, *Catal. Commun.*, 2015, **58**, 85-88; (i) J. Deutsch, J. Jiménez Pinto, S. Doerfelt, A. Martin and A. Köckritz, *Flavour Frag J.*, 2015, **30**, 101-107; (j) K. Hori, O. Ogata and W. Kuriyama, US20140163257A1, 2014; (k) S. H. Kim and S. H. Hong, *ACS Cat.*, 2014, **4**, 3630-3636; (l) K. Ding and Z. Han, WO2014059757A1, 2014; (m) N. J. Oldenhuis, V. M. Dong and Z. Guan, *Tetrahedron*, 2014, **70**, 4213-4218; (n) A. Monney, M. Pena-Lopez and M. Beller, *Chimia*, 2014, **68**, 231-234; (o) A. Monney, E. Barsch, P. Sponholz, H. Junge, R. Ludwig and M. Beller, *Chem. Commun.*, 2014, **50**, 707-709; (p) N. J. Oldenhuis, V. M. Dong and Z. Guan, *J. Am. Chem. Soc.*, 2014, **136**, 12548-12551; (q) N. T. Fairweather, M. S. Gibson and H. Guan, *Organometallics*, 2014, **34**, 335-339; (r) P. Sponholz, D. Mellmann, C. Cordes, P. G. Alsabeh, B. Li, Y. Li, M. Nielsen, H. Junge, P. Dixneuf and M. Beller, *ChemSusChem*, 2014, **7**, 2419-2422; (s) M. Nielsen, E. Alberico, W. Baumann, H.-J. Drexler, H. Junge, S. Gladiali and M. Beller, *Nature*, 2013, **495**, 85-89; (t) A. N. Marziale, A. Friedrich, I. Klopsch, M. Drees, V. R. Celinski, J. Schmedt auf der Guenne and S. Schneider, *J. Am. Chem. Soc.*, 2013, **135**, 13342-13355; (u) D. Lazzari, M. C. Cassani, M. Bertola, F. C. Moreno and D. Torrente, *RSC Adv.*, 2013, **3**, 15582-15584; (v) T. Otsuka, A. Ishii, P. A. Dub and T. Ikariya, *J. Am. Chem. Soc.*, 2013, **135**, 9600-9603; (w) A. Ishii, T. Ootsuka, M. Imamura, T. Nishimiya and K. Kimura, WO2013018573A1, 2013; (x) A. Ishii, T. Ootsuka, T. Ishimaru and M. Imamura, WO2012105431A1, 2012; (y) T. Touge, K. Aoki, H. Nara and W. Kuriyama, WO2012144650A1, 2012; (z) M. Nielsen, H. Junge, A. Kammer and M. Beller, *Angew. Chem., Int. Ed.*, 2012, **51**, 5711-5713; (aa) Z. Han, L. Rong, J. Wu, L. Zhang, Z. Wang and K. Ding, *Angew. Chem., Int. Ed. Engl.*, 2012, **51**, 13041-13045; (ab) W. Kuriyama, T. Matsumoto, O. Ogata, Y. Ino, K. Aoki, S. Tanaka, K. Ishida, T. Kobayashi, N. Sayo and T. Saito, *Org. Process Res. Dev.*, 2011, **16**, 166-171; (ac) W. Kuriyama, T. Matsumoto, Y. Ino and O. Ogata, WO2011048727A1, 2011; (ad) M. Bertoli, A. Choualeb, A. J. Lough, B. Moore, D. Spasyuk and D. G. Gusev, *Organometallics*, 2011, **30**, 3479-3482; (ae) M. Nielsen, A. Kammer, D. Cozzula, H. Junge, S. Gladiali and M. Beller, *Angew. Chem., Int. Ed.*, 2011, **50**, 9593-9597; (af) A. Staubitz, M. E. Sloan, A. P. M. Robertson, A. Friedrich, S. Schneider, P. J. Gates, J. Schmedt auf der Gunne and I. Manners, *J. Am. Chem. Soc.*, 2010, **132**, 13332-13345; (ag) M. Käß, A. Friedrich, M. Drees and S. Schneider, *Angew. Chem., Int. Ed.*, 2009, **48**, 905-907; (ah) A. Friedrich, M. Drees and S. Schneider, *Chem. - Eur. J.*, 2009, **15**, 10339-10342.
7. (a) S. T. Ahn, E. A. Bielinski, E. M. Lane, Y. Chen, W. H. Bernskoetter, N. Hazari and G. T. R. Palmore, *Chem. Commun.*, 2015, **51**, 5947-5950; (b) K. Junge, B. Wendt, H. Jiao and M. Beller, *ChemCatChem*, 2014, **6**, 2810-2814; (c) M. Pera-Titus and F. Shi, *ChemSusChem*, 2014, **7**, 720-722; (d) T. J. Schmeier, G. E. Dobereiner, R. H. Crabtree and N. Hazari, *J. Am. Chem. Soc.*, 2011, **133**, 9274-9277; (e) T. W. Graham, C.-W. Tsang, X. Chen, R. Guo, W. Jia, S.-M. Lu, C. Sui-Seng, C. B. Ewart, A. Lough, D. Amoroso and K. Abdur-Rashid, *Angew. Chem., Int. Ed.*, 2010, **49**, 8708-8711, S8708/8701-S8708/8711; (f) N. Andrushko, V. Andrushko, P. Roose, K. Moonen and A. Börner, *ChemCatChem*, 2010, **2**, 640-643; (g) X. Chen, W. Jia, R. Guo, T. W. Graham, M. A. Gullons and K. Abdur-Rashid, *Dalton Trans.*, 2009, 1407-1410; (h) K. Abdur-Rashid, R. Guo, X. Chen and W. Jia, US20080300430A1, 2008; (i) Z. E. Clarke, P. T. Maragh, T. P. Dasgupta, D. G. Gusev, A. J. Lough and K. Abdur-Rashid, *Organometallics*, 2006, **25**, 4113-4117; (j) K. Abdur-Rashid, US20050107638A1, 2005; (k) K. Abdur-Rashid, WO2004096735A2, 2004.
8. S. Chakraborty, O. Blacque, T. Fox and H. Berke, *Chem. – Asian J.*, 2014, **9**, 328-337.
9. P. A. Dub, B. L. Scott and J. C. Gordon, *Organometallics*, 2015, **34**, 4464-4479.
10. P. A. Dub; J. C. Gordon, (a) International Patent Application PCT/US2015/034793, 2015; (b) US Provisional Patent Applications: 1) 62/136,085, 2015; 2) 62/130,977, 2015; 3) 62/009,483, 2014.
11. H. Pellissier, *Chiral Sulfur Ligands, Asymmetric Catalysis*, Royal Society of Chemistry Publishing, 2009.

12. H. Shimizu, I. Nagasaki, K. Matsumura, N. Sayo and T. Saito, *Acc. Chem. Res.*, 2007, **40**, 1385-1393.
13. R. M. Bullock, *Catalysis Without Precious Metals*, Wiley-Blackwell, 2010.
14. (a) A. J. Rucklidge, D. S. McGuinness, R. P. Tooze, A. M. Z. Slawin, J. D. A. Pelletier, M. J. Hanton and P. B. Webb, *Organometallics*, 2007, **26**, 2782-2787; (b) D. S. McGuinness, D. B. Brown, R. P. Tooze, F. M. Hess, J. T. Dixon and A. M. Z. Slawin, *Organometallics*, 2006, **25**, 3605-3610.
15. (a) P. J. Bonitatibus, Jr., S. Chakraborty, M. D. Doherty, O. Siclovan, W. D. Jones and G. L. Soloveichik, *Proc. Natl. Acad. Sci. U. S. A.*, 2015, **112**, 1687-1692; (b) L. S. Sharninghausen, B. Q. Mercado, R. H. Crabtree and N. Hazari, *Chem. Commun.*, 2015, **51**, 16201-16204; (c) N. T. Fairweather, M. S. Gibson, H. Guan, S. Chakraborty, H. Dai and P. Bhattacharya, US20150274621A1, 2015; (d) J. Quintaine and L. Saudan, WO2015091158A1, 2015; (e) M. Peña-López, H. Neumann and M. Beller, *ChemCatChem*, 2015, **7**, 865-871; (f) E. A. Bielinski, M. Forster, Y. Zhang, W. H. Bernskoetter, N. Hazari and M. C. Holthausen, *ACS Catal.*, 2015, **5**, 2404-2415; (g) S. Chakraborty, H. Dai, P. Bhattacharya, N. T. Fairweather, M. S. Gibson, J. A. Krause and H. Guan, *J. Am. Chem. Soc.*, 2014, **136**, 7869-7872; (h) E. A. Bielinski, P. O. Lagaditis, Y. Zhang, B. Q. Mercado, C. Würtele, W. H. Bernskoetter, N. Hazari and S. Schneider, *J. Am. Chem. Soc.*, 2014, **136**, 10234; (i) S. Chakraborty, W. W. Brennessel and W. D. Jones, *J. Am. Chem. Soc.*, 2014, **136**, 8564-8567; (j) S. Werkmeister, K. Junge, B. Wendt, E. Alberico, H. Jiao, W. Baumann, H. Junge, F. Gallou and M. Beller, *Angew. Chem., Int. Ed.*, 2014, **53**, 8722-8726; (k) S. Chakraborty, P. O. Lagaditis, M. Förster, E. A. Bielinski, N. Hazari, M. C. Holthausen, W. D. Jones and S. Schneider, *ACS Catal.*, 2014, **4**, 3994-4003; (l) S. Qu, H. Dai, Y. Dang, C. Song, Z.-X. Wang and H. Guan, *ACS Catal.*, 2014, **4**, 4377-4388; (m) P. Dupau, M.-L. Tran Do, S. Gaillard and J.-L. Renaud, *Angew. Chem., Int. Ed.*, 2014, **53**, 13004-13006; (n) C. Bornschein, S. Werkmeister, B. Wendt, H. Jiao, E. Alberico, W. Baumann, H. Junge, K. Junge and M. Beller, *Nat. Commun.*, 2014, **5**, 4111; (o) E. Alberico, P. Sponholz, C. Cordes, M. Nielsen, H.-J. Drexler, W. Baumann, H. Junge and M. Beller, *Angew. Chem., Int. Ed.*, 2013, **52**, 14162-14166.
16. (a) R. Xu, S. Chakraborty, H. Yuan and W. D. Jones, *ACS Catal.*, 2015, **5**, 6350-6354; (b) G. Zhang, K. V. Vasudevan, B. L. Scott and S. K. Hanson, *J. Am. Chem. Soc.*, 2013, **135**, 8668-8681; (c) G. Zhang and S. K. Hanson, *Org. Lett.*, 2013, **15**, 650-653; (d) G. Zhang and S. K. Hanson, *Chem. Commun.*, 2013, **49**, 10151-10153; (e) G. Zhang, B. L. Scott and S. K. Hanson, *Angew. Chem., Int. Ed.*, 2012, **51**, 12102-12106; (f) L. Chen, P. Ai, J. Gu, S. Jie and B.-G. Li, *J. Organomet. Chem.*, 2012, **716**, 55-61; (g) S. Jie, B. Li, L. Chen and P. Ai, CN102659961A, 2012.
17. K. V. Vasudevan, B. L. Scott and S. K. Hanson, *Eur. J. Inorg. Chem.*, 2012, **2012**, 4898-4906.
18. M. D. Fryzuk, D. B. Leznoff, R. C. Thompson and S. J. Rettig, *J. Am. Chem. Soc.*, 1998, **120**, 10126-10135.
19. (a) S. Chakraborty, P. Bhattacharya, H. Dai and H. Guan, *Acc. Chem. Res.*, 2015, **48**, 1995-2003; (b) Y.-Y. Li, S.-L. Yu, W.-Y. Shen and J.-X. Gao, *Acc. Chem. Res.*, 2015, **48**, 2587-2598; (c) B. Su, Z.-C. Cao and Z.-J. Shi, *Acc. Chem. Res.*, 2015, **48**, 886-896; (d) P. J. Chirik, *Acc. Chem. Res.*, 2015, **48**, 1687-1695; (e) R. M. Bullock and M. L. Helm, *Acc. Chem. Res.*, 2015, **48**, 2017-2026; (f) R. H. Morris, *Acc. Chem. Res.*, 2015, **48**, 1494-1502.
20. (a) B. Askevold, M. M. Khusniyarov, W. Kroener, K. Gieb, P. Mueller, E. Herdtweck, F. W. Heinemann, M. Diefenbach, M. C. Holthausen, V. Vieru, L. F. Chibotaru and S. Schneider, *Chem. - Eur. J.*, 2015, **21**, 579-589; (b) A. Glueer, B. Askevold, B. Schlusshass, F. W. Heinemann and S. Schneider, *Z. Anorg. Allg. Chem.*, 2015, **641**, 49-51; (c) B. Askevold, J. T. Nieto, S. Tussupbayev, M. Diefenbach, E. Herdtweck, M. C. Holthausen and S. Schneider, *Nat. Chem.*, 2011, **3**, 532-537; (d) B. Askevold, M. M. Khusniyarov, E. Herdtweck, K. Meyer and S. Schneider, *Angew. Chem., Int. Ed.*, 2010, **49**, 7566-7569; (e) A. Friedrich, M. Drees, M. Kaess, E. Herdtweck and S. Schneider, *Inorg. Chem.*, 2010, **49**, 5482-5494; (f) A. Friedrich, M. Drees, J. Schmedt auf der Guenne and S.

- Schneider, *J. Am. Chem. Soc.*, 2009, **131**, 17552-17553; (g) M. Kaess, A. Friedrich, M. Drees and S. Schneider, *Angew. Chem., Int. Ed.*, 2009, **48**, 905-907.
21. (a) I. Koehne, T. J. Schmeier, E. A. Bielinski, C. J. Pan, P. O. Lagaditis, W. H. Bernskoetter, M. K. Takase, C. Wuertele, N. Hazari and S. Schneider, *Inorg. Chem.*, 2014, **53**, 2133-2143; (b) K. L. Fillman, E. A. Bielinski, T. J. Schmeier, J. C. Nesvet, T. M. Woodruff, C. J. Pan, M. K. Takase, N. Hazari and M. L. Neidig, *Inorg. Chem.*, 2014, **53**, 6066-6072.
22. (a) M. Kinauer, M. G. Scheibel, J. Abbenseth, F. W. Heinemann, P. Stollberg, C. Wuertele and S. Schneider, *Dalton Trans.*, 2014, **43**, 4506-4513; (b) B. Askevold, A. Friedrich, M. R. Buchner, B. Lewall, A. C. Filippou, E. Herdtweck and S. Schneider, *J. Organomet. Chem.*, 2013, **744**, 35-40; (c) M. G. Scheibel, I. Klopsch, H. Wolf, P. Stollberg, D. Stalke and S. Schneider, *Eur. J. Inorg. Chem.*, 2013, **2013**, 3836-3839; (d) M. G. Scheibel, B. Askevold, F. W. Heinemann, E. J. Reijerse, B. de Bruin and S. Schneider, *Nat. Chem.*, 2012, **4**, 552-558; (e) J. Meiners, M. G. Scheibel, M.-H. Lemee-Cailleau, S. A. Mason, M. B. Boeddinghaus, T. F. Faessler, E. Herdtweck, M. M. Khusniyarov and S. Schneider, *Angew. Chem., Int. Ed.*, 2011, **50**, 8184-8187; (f) A. Friedrich, R. Ghosh, R. Kolb, E. Herdtweck and S. Schneider, *Organometallics*, 2009, **28**, 708-718; (g) J. Meiners, A. Friedrich, E. Herdtweck and S. Schneider, *Organometallics*, 2009, **28**, 6331-6338.
23. (a) A. N. Marziale, E. Herdtweck, J. Eppinger and S. Schneider, *Inorg. Chem.*, 2009, **48**, 3699-3709; (b) M. Ines Garcia-Seijo, A. Habtemariam, S. Parsons, R. O. Gould and M. Esther Garcia-Fernandez, *New J. Chem.*, 2002, **26**, 636-644; (c) M. I. Garcia-Seijo, A. Habtemariam, D. Fernandez-Anca, S. Parsons and M. E. Garcia-Fernandez, *Z. Anorg. Allg. Chem.*, 2002, **628**, 1075-1084; (d) M. M. T. Khan and E. R. Rao, *Polyhedron*, 1987, **6**, 1727-1735.
24. (a) I. Klopsch, M. Finger, C. Wuertele, B. Milde, D. B. Werz and S. Schneider, *J. Am. Chem. Soc.*, 2014, **136**, 6881-6883; (b) M. G. Scheibel, Y. Wu, A. C. Stueckl, L. Krause, E. Carl, D. Stalke, B. de Bruin and S. Schneider, *J. Am. Chem. Soc.*, 2013, **135**, 17719-17722.
25. A. Choualeb, A. J. Lough and D. G. Gusev, *Organometallics*, 2007, **26**, 3509-3515.
26. (a) S. S. Rozenel, R. Padilla and J. Arnold, *Inorg. Chem.*, 2013, **52**, 11544-11550; (b) S. S. Rozenel, R. Padilla, C. Camp and J. Arnold, *Chem. Commun.*, 2014, **50**, 2612-2614; (c) C. Camp, L. C. E. Naested, K. Severin and J. Arnold, *Polyhedron*, 2015, DOI: 10.1016/j.poly.2015.09.001, Ahead of Print.
27. A. A. Danopoulos, P. G. Edwards, J. S. Parry and A. R. Wills, *Polyhedron*, 1989, **8**, 1767-1769.
28. (a) M. Kacan, M. Turkeyilmaz, F. Karabulut, O. Altun and Y. Baran, *Spectrochim. Acta A*, 2014, **118**, 572-577; (b) P. G. Alsabeh, R. McDonald and M. Stradiotto, *Organometallics*, 2012, **31**, 1049-1054.
29. G. A. Bain and J. F. Berry, *J. Chem. Educ.*, 2008, **85**, 532.
30. K. Burger, *Coordination chemistry: experimental methods*, CRC Press, 1973.
31. (a) W. Kohn and L. J. Sham, *Phys. Rev.*, 1965, **140**, A1133-A1138; (b) P. Hohenberg and W. Kohn, *Phys. Rev.*, 1964, **136**, B864-B871.
32. J.-D. Chai and M. Head-Gordon, *Phys. Chem. Chem. Phys.*, 2008, **10**, 6615-6620.
33. (a) J. M. L. Martin and A. Sundermann, *J. Chem. Phys.*, 2001, **114**, 3408-3420; (b) M. Dolg, U. Wedig, H. Stoll and H. Preuss, *J. Chem. Phys.*, 1987, **86**, 866-872.
34. M. J. Frisch, G. W. Trucks, H. B. Schlegel, G. E. Scuseria, M. A. Robb, J. R. Cheeseman, G. Scalmani, V. Barone, B. Mennucci, G. A. Petersson, H. Nakatsuji, M. Caricato, X. Li, H. P. Hratchian, A. F. Izmaylov, J. Bloino, G. Zheng, J. L. Sonnenberg, M. Hada, M. Ehara, K. Toyota, R. Fukuda, J. Hasegawa, M. Ishida, T. Nakajima, Y. Honda, O. Kitao, H. Nakai, T. Vreven, J. A. Montgomery, Jr., J. E. Peralta, F. Ogliaro, M. Bearpark, J. J. Heyd, E. Brothers, K. N. Kudin, V. N. Staroverov, T. Keith, R. Kobayashi, J. Normand, K. Raghavachari, A. Rendell, J. C. Burant, S. S. Iyengar, J. Tomasi, M. Cossi, N. Rega, J. M. Millam, M. Klene, J. E. Knox, J. B. Cross, V. Bakken, C. Adamo, J. Jaramillo, R. Gomperts, R. E. Stratmann, O. Yazyev, A. J. Austin, R. Cammi, C. Pomelli, J. W. Ochterski, R. L. Martin, K. Morokuma, V. G. Zakrzewski, G. A. Voth, P. Salvador, J. J.

- Dannenberg, S. Dapprich, A. D. Daniels, O. Farkas, J. B. Foresman, J. V. Ortiz, J. Cioslowski, and D. J. Fox, Gaussian, Inc., Wallingford CT, 2013.
35. E. F. Pettersen, T. D. Goddard, C. C. Huang, G. S. Couch, D. M. Greenblatt, E. C. Meng and T. E. Ferrin, *J. Comp. Chem.*, 2004, **25**, 1605-1612.
  36. Both cobalt(II) complexes **3** and **4**, on the contrary to iron(II) complex **2**, are visually air-stable in both solid-state and in solution.
  37. K. L. Fillman, E. A. Bielinski, T. J. Schmeier, J. C. Nesvet, T. M. Woodruff, C. J. Pan, M. K. Takase, N. Hazari and M. L. Neidig, *Inorg. Chem.*, 2014, **53**, 6066-6072.
  38. The computed structure **4B** in the gas-phase is geometrically different with respect to the N(H)-Co-Cl<sub>2</sub> angle derived from the structure of **4** in the solid-state (X-Ray). This difference is likely attributable to packing effects in the solid-state structure.
  39. S. D. Holt, B. Piggott, M. B. Hursthouse and R. L. Short, *Polyhedron*, 1987, **6**, 1457-1461.
  40. D. Walther, T. Döhler, K. Heubach, O. Klobes, B. Schweder and H. Görls, *Z. Anorg. Allg. Chem.*, 1999, **625**, 923-932.
  41. (a) Y. Funahashi, C. Kato and O. Yamauchi, *Bull. Chem. Soc. Jpn.*, 1999, **72**, 415-424; (b) D. E. Nikles, M. J. Powers and F. L. Urbach, *Inorg. Chim. Acta*, 1979, **37**, L499-L501; (c) V. M. Miskowski, J. A. Thich, R. Solomon and H. J. Schugar, *J. Am. Chem. Soc.*, 1976, **98**, 8344-8350.
  42. E. L. Klein, M. A. Khan and R. P. Houser, *Inorg. Chem.*, 2004, **43**, 7272-7274.
  43. (a) M. Xie, G. Zhu, Y. Hu and H. Gu, *J. Phys. Chem. C*, 2011, **115**, 20596-20602; (b) A. L. Capparelli, J. Marañon, O. M. Sorarrain and R. R. Filgueria, *J. Mol. Struct.*, 1974, **23**, 145-151.

